Check for updates

Advances in Materials Technology for Fossil Power Plants
Proceedings from the Eighth International Conference
October 11–14, 2016, Albufeira, Algarve, Portugal
https://doi.org/10.31399/asm.cp.am-epri-2016p0989

Copyright © 2016 ASM International®. All rights reserved.
J. Parker, J. Shingledecker, J. Siefert, editors

EXPERIENCE WITH 9Cr3W3CoVNbBN STEEL IN TERMS OF WELDING, CREEP AND OXIDATION

K. G. Abstoss, A. Nitsche, P. Mayr
Institute of Joining and Assembly, Technische Universität Chemnitz, Germany

C. Schlacher
Institute of Materials Science and Welding, Graz University of Technology, Austria

V. González, A. Agüero
National Institute for Aerospace Technology INTA, Spain

ABSTRACT

The presented work summarizes the results of more than 10 years of research at TU Graz and TU Chemnitz and partners on a martensitic boron and nitrogen stabilized 9Cr3W3Co (MARBN) steel grade. The design philosophy of MARBN steels is presented and critical issues regarding boron and nitrogen balance are discussed. Microstructural characterization of two different laboratory heats, is presented and efforts in European projects towards an upscaling of melts are presented. Base material creep testing data at 650 °C up to 50.000 hours is presented and assessed to commercial alloys such as ASTM grades P91 and P92. An increase of creep rupture stress of more than +20% was recorded. Oxidation tests in steam at 650°C revealed an anomalous response of the material. Several specimens exhibited excellent oxidation resistance commonly only seen for grades of higher chromium content. The anomalous oxidation behaviour is identified and discussed, although the causes remain yet unclear. Results of manufacturing, characterization and testing of different MARBN welds, including gas-tungsten-arc-, gas-metal-arc-, friction stir and electron beam welds reveal a microstructure memory effect in the heat affected zone, so that no uniform fine-grained zone is present. The behaviour of crosswelds during long-term creep testing at 650 °C up to more than 32.000 hours is assessed and the susceptibility to Type IV cracking is discussed. The manuscript summarizes research of more than 10 years, presents current research activities on MARBN and describes open questions for an alloy identified as a promising martensitic steel grade for elevated temperature components.

INTRODUCTION

Despite the undeniable driving force to promote the use of alternative energy sources caused by CO_2 – pollution and global warming there will still be a strong need of thermal power plants in the future. Due to the world wide increasing demand of energy especially the coal-fired power plants will play an important role securing a low-cost base electricity supply. However, traditional coal-fired power plants are intensive sources of the global CO_2 emissions [1]. One way to reduce the emissions is to improve the net efficiency of the power plant by increasing the temperature and pressure in the steam cycle [2]. Over the last decades there was a significant increase in steam conditions resulting in so called supercritical power plants acting at temperatures of 600-620 °C and pressures up to 300 bar. This substantial progress from subcritical (540 °C/180 bar) to supercritical conditions leads to an increase in relative efficiency of 6.5 % and a corresponding reduction in specific CO_2 emissions of 30 % [3, 4, 6, 9, 15]. These operating conditions impose advanced requirements on the materials. A further increase in steam parameters is limited by the

Downloaded from http://dl.asminternational.org/am-epri/proceedings-pdf/AM-EPRI2016/84673/989/678749/epri2016p0989.pdf
by guest

properties of the application materials [7, 8]. Advanced 9-12 % Cr ferritic/martensitic steels were found as one of the key candidates for high temperature applications in thermal power plants due to their excellent properties. Such steel grades offer a good combination of acceptable steam oxidation and corrosion resistance, high creep strength and good manufacturability [3, 10-12, 15]. For that reason, 9 % Cr (wt. %) ferritic/martensitic steels such as P91, P92 and E911 are already widely used for high temperature components in fossil- fired power plants and due to their high potential, they have been made subject of serious materials development in the last decades [3-6]. The alloy development of these heat resistant steels is strongly motivated to both the economic and environmental perspective to enhance the steam parameters in fossil fired power plants in order to further increase thermal efficiency and reduce CO_2 emissions. One of these very promising 9 % Cr candidates for future high efficient power plant applications is based on a special alloying concept called MARBN [9, 13, 14]. These **mar**tensitic steels strengthened by **b**oron and **n**itrogen were targeting an enhancement of creep resistance by stabilizing the microstructure through precise amounts of boron and nitrogen. The present work summarizes results of several years of research on the MARBN steel grade with regards to creep performance, welding behaviour and oxidation issues.

EXPERIMENTAL

Alloy Design Philosophy

The alloy concept of MARBN, developed by the national institute for material science (NIMS) is mainly targeting on enhancing creep strength of both the base materials and welded joints. This is mainly reached by combining a solid solution strengthening effect of boron and precipitation hardening by fine MX carbonitrides which enhances the sub-boundary hardening [9,16].

By adding nitrogen, densely distributed vanadium/niobium rich carbonitrides precipitate along the martensite packet, block and lath boundaries as well as at the prior austenite grain boundaries (PAGB). These nano-sized MX particles act as obstacles to the boundaries and to the dislocation movement, which reduces the recovery during creep exposure leading to an increase of the creep strength [9, 21].

Systematic investigations showed that the controlled addition of boron leads to a significant improvement of creep strength by enriching the $M_{23}C_6$ carbides [9, 17, 18]. During the normalizing heat treatment a segregation of boron at the grain boundaries takes place. A subsequent tempering treatment leads to the preferential precipitation of $M_{23}(C,B)_6$ particles at the prior austenite grain boundaries (PAGB) and martensite sub-boundaries and an enrichment of boron in $M_{23}C_6$ to form $M_{23}(CB)_6$ in the vicinity of the PAGB. This enrichment decreases the coarsening rate of the $M_{23}C_6$ carbides near the PAGB during creep service [9, 17, 19].

In order to ensure the creep strengthening effects of boron and nitrogen it is necessary to strictly balance the alloyed amount. Based on experimental investigations regarding the solubility of boron and nitrogen the ratio should be adjusted considering following equation:

$$\log[\%B] = -2.45 \log[\%N] - 6.81$$

With [%B] and [%N] as the soluble wt. % concentrations of boron and nitrogen there is a maximum nitrogen concentration of e.g. 95 ppm where 139 ppm boron can dissolve in the matrix [9, 17, 18]. Excessive addition of boron in combination with nitrogen over the solid solubility relation promotes the formation of coarse boron nitrides (BN) leading to a loss of the benefitial strengthening effect caused by a decreasing amount of solute boron and nitrogen [9, 16, 17].

Downloaded from http://dl.asminternational.org/am-epri/proceedings-pdf/AM-EPRI2016/84673/989/678749/epri2016p0989.pdf
by guest

Beside the long term creep strengthening effect of boron due to reduction of $M_{23}C_6$ particle coarsening, there is another beneficial effect with regards to the creep strength of welded joints. The addition of boron affects the α/γ transformation during the weld thermal cycle and leads to a suppression of the fine-grained heat affected zone (FGHAZ). Instead the average grain size of the heat affected zone (HAZ) and of the base material appears to substantially be the same. Abe et al. showed that the grain boundary segregation of boron reduces the interfacial boundary energy, which makes these grain boundaries less effective as nucleation sites for the austenite phase leading to a suppression of subsequent recrystallization during the weld thermal cycle [17]. The effect of retarding the diffusive α/γ transformation and reproducing the same grain size and orientation as the original austenite is called α/γ reverse transformation and has been discussed by several authors [17, 20-22]. Type IV cracking as a typical failure mechanisms of 9-12 % Cr welded joints could be avoided by the suppression of a distinctive FGHAZ resulting in an improved cross-weld creep performance.

Materials

Based on the alloy design philosophy, two experimental laboratory heats MARBN 1 (20 kg) and MARBN 2 (100 kg) were produced by vacuum induction melting. The 20 kg MARBN 1 heat was forged to a final dimension of 50 mm x 50 mm. Heat MARBN 2 was forged and hot rolled to plates of 20 mm of thickness. Both MARBN heats were normalized for one hour at 1150 °C followed by a subsequent four hour tempering treatment at 770 °C and air cooling. The resulting chemical composition in weight % of the MARBN heats as well as that of the P92 benchmark material is given in Table 1.

Table 1: Chemical composition of two investigated 9Cr3W3CoVNbBN heats in wt. % (balance: Fe).

Analysis	C	Si	Mn	Cr	Ni	W	V	Nb	Co	Al	B	N
MARBN1	0.074	0.3	0.4	9.26	0.06	2.84	0.21	0.056	2.95	<0.005	0.0120	0.0130
MARBN2	0.090	0.3	0.5	9.26	-	2.92	0.20	0.050	2.88	0.004	0.0114	0.0100
P92	0.12	0.1	0.6	9.37	-	1.98	0.23	-	-	-	-	0.04

Oxidation Testing

MARBN 1 specimens were taken from a forged ingot [23]. The schematics of the closed loop laboratory rig employed at INTA are shown elsewhere [24]. Prior to testing, laboratory air is displaced from the specimen chamber by means of N_2 which is kept flowing while heating up to the test temperature (approximately at a rate of 600 ºC/h). Once the test temperature has been reached, the N_2 flow is stopped and pure steam is introduced at a linear velocity of 8 cm/s. To carry out weight measurements or to remove samples, the furnace is cooled to about 300 ºC under N_2 atmosphere and the specimens are subsequently removed. The reheat cycle is also carried out under N_2 atmosphere. The oxidized specimens were characterized by light optical microscopy (Leica MEF 4) and field emission scanning electron microscopy (FESEM) employing a JEOL JSM 840 system equipped with an energy dispersive X-ray spectrometer (EDS) KEVEX MICROANALYST 8000 with a RÖNTEC signal processor.

Welding Procedure

In the course of welding investigations several welded joints were fabricated using four different welding procedures. The MARBN 1 heat was welded by the gas tungsten arc welding (GTAW)

Downloaded from http://dl.asminternational.org/am-epri/proceedings-pdf/AM-EPRI2016/84673/989/678749/epri2016p0989.pdf
by guest

process. For this joint the material was welded using a nickel based filler metal (NIBAS 70/20-IG). Three more welding procedures were applied on the other heat MARBN 2 including of gas metal arc welding (GMAW), friction stir welding (FSW) and electron beam welding (EBW), respectively. The GMAW was carried out using a chemically matching flux cored wire. FSW welding was selected as a procedure for solid state and low heat input welding, using a tungsten-lanthanum oxide tool. EBW technique was selected for comparison reason ensuring a narrow HAZ. After each welding procedure a final post-weld heat treatment at 740 °C was carried out for a duration of four hours.

Creep testing

In order to evaluate the creep behaviour of the base material and the cross-welds at different stress levels specimens were manufactured according to Fig. 1 (left). The cross-weld specimens were machined perpendicular to the welding direction, resulting in creep specimens composed of weld metal, HAZ and base metal as shown in Fig. 1 right. The testing stress levels of 60 to 150 MPa result from the different gauge diameter dimension of each specimen. Uniaxial creep tests were carried out at 650 °C according to the EN ISO 204:2009 standard using a vertical dead-weight creep testing machine.

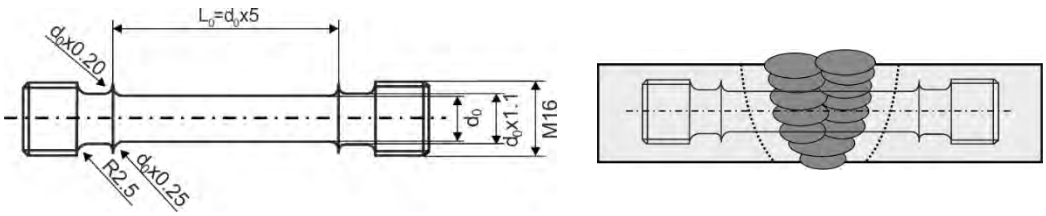


Figure 1: Technical drawing of creep specimen according to EN ISO 204:2009 (left) and schematic drawing of cross-weld specimens extraction (right).

RESULTS

Base Material Microstructure

Microstructural observations using electron microscopy revealed the typical martensitic structure of these MARBN steel grades. Figure 2 (left) shows the inverse pole figure map obtained by electron backscatter diffraction (EBSD) method. The martensite laths and laths packages as well as the PAGB of the MARBN 2 heat in tempered condition are clearly visible. The martensitic microstructure consists of different kinds of precipitates, aligning along the PAGB and martensite lath boundaries, respectively. Figure 2 (middle) shows these various precipitates after the quality heat treatment of MARBN 2. The smaller precipitates located within the matensite substructure are found as vanadium and niobium rich carbonitrides. The coarse precipitates which were aligned along the PAGB were identified as $M_{23}C_6$ chromium-rich carbides. These carbides and carbonitrides enhancing the boundary and sub-boundary hardening make a substantial contribution to the strengthening effect according to the MARBN design philosophy. As described, the boron and nitrogen concentration has to be adjusted precisely in the range of few ppm to suppress the formation of boron nitrides and ensure the solid solution boron strengthening. Figure 2 (right) shows a SEM image of detected boron nitrides located in the dimples of the MARBN 1 tensile fracture plane. With contents of 120 ppm boron and 130 ppm nitrogen, respectively the solubility of these elements within the MARBN 1 matrix is not guaranteed. This results in the formation of boron nitrides, showing diameters of about 1-2 μm.

Downloaded from http://dl.asminternational.org/am-epri/proceedings-pdf/AM-EPRI2016/84673/989/678749/epri2016p0989.pdf
by guest

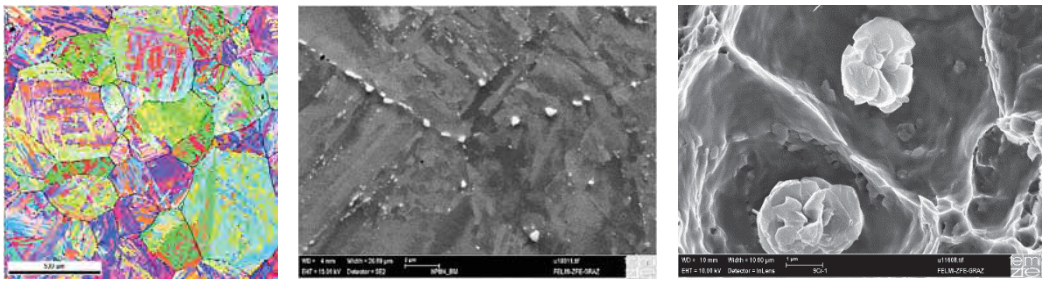


Figure 2: Electron micoscopy of the microstructure of MARBN 2 using EBSD (left) and SEM (middle) as well as representative boron nitrides of MARBN 1 (right).

Oxidation Testing

The mass variation of MARBN 1 specimens as a function of exposure time at 650 ºC under flowing steam is shown in Fig. 3. The oxidation rate of P92 was also included in the test for comparison purposes. Specimen preparation consisted of degreasing and grinding (120 grit) prior to exposure.

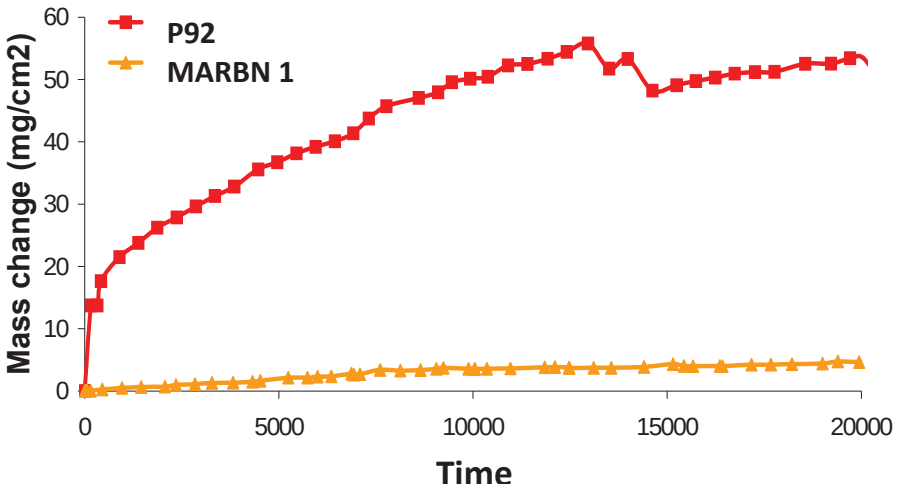
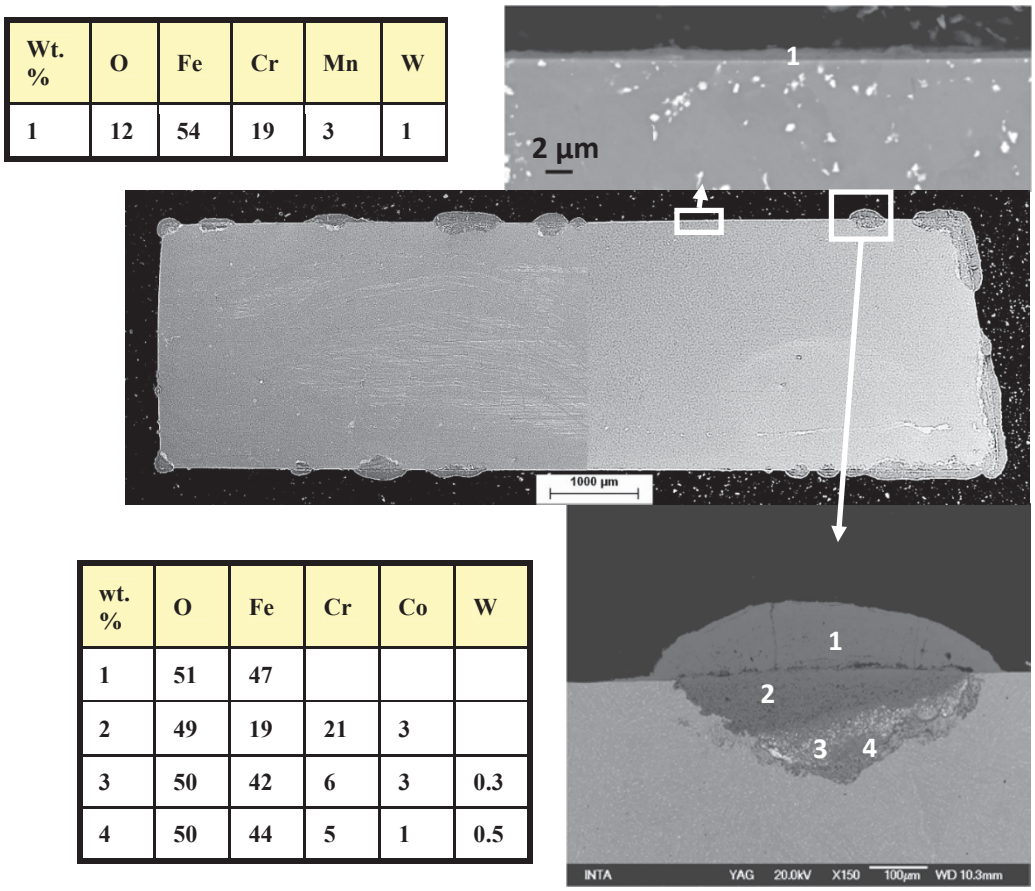


Figure 3: Mass variation of MARBN 1 and P92 exposed to pure steam at 650 °C.

As shown, the ground specimen displayed very low weight gain in particular when compared to 9 Cr (wt. %) P92. Except for the sample's edges, most of the surface of the specimen exposed for 20.000 h was covered with a very thin Cr rich protective oxide layer. Some thicker oxide nodules were also present, likely as a result of defects present in the protective layer from the very beginning of the exposure (Fig. 4) [23]. The nodules consist of a thick dual layered oxide scale, very similar to that observed on P92 and characteristic for 9 Cr (wt. %) ferritic steels [25]. It consists of a top outwards growing Fe_3O_4 layer and an inwards growing mixed oxide layer containing $(Fe, Cr)_3O_4$, FeO and Cr_2O_3 as well as other elements present in the substrate such as Co and W. These nodules are present from the beginning of the oxidation test and grow both sidewise and in thickness but no new nodules appear to develop.

Downloaded from http://dl.asminternational.org/am-epri/proceedings-pdf/AM-EPRI2016/84673/989/678749/epri2016p0989.pdf
by guest

Wt. %	O	Fe	Cr	Mn	W
1	12	54	19	3	1



wt. %	O	Fe	Cr	Co	W
1	51	47			
2	49	19	21	3	
3	50	42	6	3	0.3
4	50	44	5	1	0.5

Figure 4: MARBN 1 specimen exposed for 20.000 h to pure steam at 650 ºC.

The development of the thin protective oxide, rich in Cr as well as in Mn, can be attributed to the presence of a very fine grained zone beneath the scale [23]. However, it is not clear yet why this zone is formed on MARBN and not in other 9 wt. % Cr steels, such as P92 undergoing the same grinding process. This protective oxide grows slowly as can be seen in Fig. 5, where cross sections of samples exposed to 5.000, 10.000 and 20.000 h are shown, reaching only 1 µm after 20.000 h of exposure.

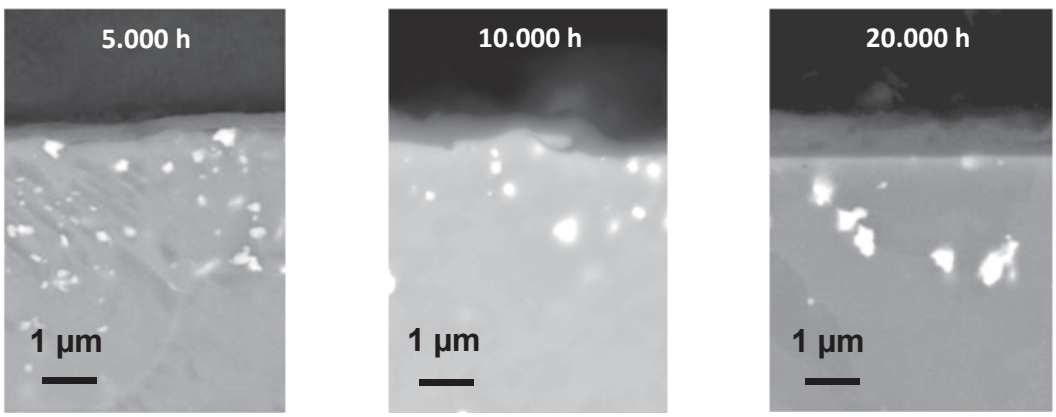


Figure 5: FESEM cross sections of MARBN 1 specimens exposed to pure steam at 650 ºC.

Downloaded from http://dl.asminternational.org/am-epri/proceedings-pdf/AM-EPRI2016/84673/989/678749/epri2016p0989.pdf
by guest

Welding Procedure

Figure 6 shows light optical images of each welded joint of the MARBN 1 and MARBN 2 heat. With regards to the welding procedure there occured no difficulties during the four different welding tests. All four joints were successfully produced without any defects or cracks. Furthermore, light optical investigations as well as EBSD measurements revealed a successfully suppressed fine-grained heat affected zone. This is exemplified by the EBSD measurements of the GMAW weld in Fig. 7 exhibiting a detailed view of the heat affected zone as well as the weld metal and base metal. Comparing the EBSD results of the base metal and the heat affected zone it can be clearly seen that there is no uniform fine-grained zone. The microstructure of this area shows a formation of small grains aligning along the prior austentite grain boundaries instead. This formation of the HAZ microstructure was observed at all four welded joints regardless of the welding procedure. Based on the fact of the mentioned α/γ reverse transformation an uniform grain refinement in this HAZ region is successfully suppressed.

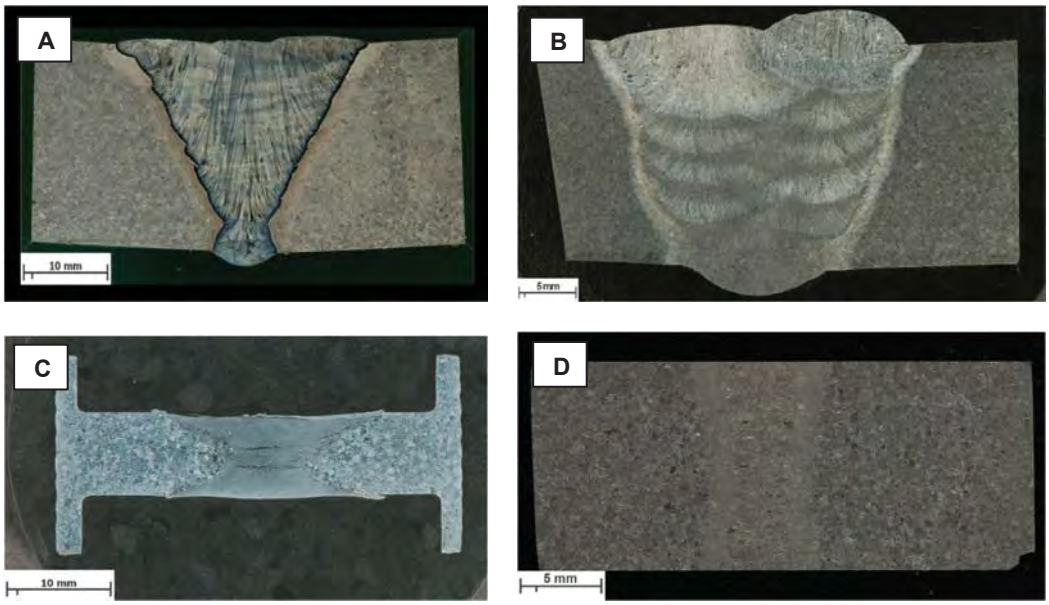


Figure 6: Light optical images of the microstructure of MARBN 1 GTAW weld (A) and MARBN 2 GMAW (B), FSW (C) and EBW welds (D) [28].

Downloaded from http://dl.asminternational.org/am-epri/proceedings-pdf/AM-EPRI2016/84673/989/678749/epri2016p0989.pdf
by guest

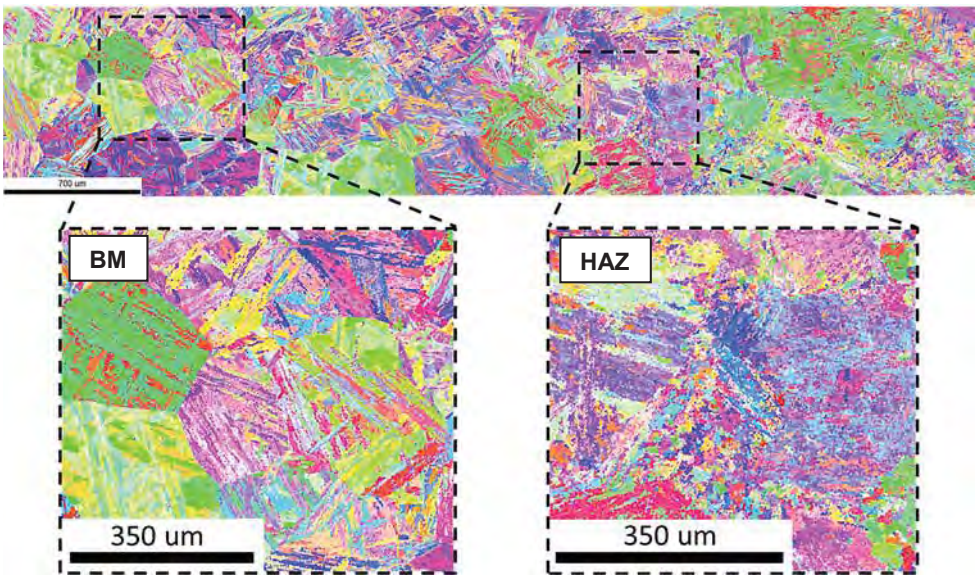


Figure 7: EBSD measurements of the GMAW welded joint, showing the base metal (BM) and the heat affected zone (HAZ) [27].

Creep Behaviour

Figure 8 shows the creep data of the two MARBN heats (left) and their welded joints (right). It can be seen that both base materials, MARBN 1 and MARBN 2 exhibit significant improved creep strength in comparison to the P92 base material [26]. At higher stress levels there is no big difference in the creep strength of the MARBN heats. At a stress level of 100 MPa MARBN heat 1 exibits 23.997 h while the MARBN 2 creep specimen is still running showing 48.945 h. Taking the observed boron nitrides of the MARBN 1 heat into account this drop in creep strength is reasonable. The existence of boron nitrides leads to a reduction of the beneficial strengthening effect due to the decreasing solute content of boron and nitrogen, which results in a reduced time to rupture at lower stress levels.

Figure 8 right shows the creep test data for the MARBN 1 and MARBN 2 crosswelds compared to the well established grade 92 base material [26] and welded joints [29]. The creep tests revealed the following:

- All crossweld samples could not reach the time to rupture values of the MARBN 2 base material
- At higher stress levels, the creep strength of the crosswelds is still on a higher level compared to grade 92 base material and on a much higher level compared to grade 92 welded joints.
- At lower stress levels, a significant drop in creep life for the GTAW and GMAW crosswelds was observed.
- The FSW crosswelds do not show an increase in creep strength compared to GTAW and GMAW crosswelds.
- The EBW crosswelds showed the best results of all welded joints.

Downloaded from http://dl.asminternational.org/am-epri/proceedings-pdf/AM-EPRI2016/84673/989/678749/epri2016p0989.pdf
by guest

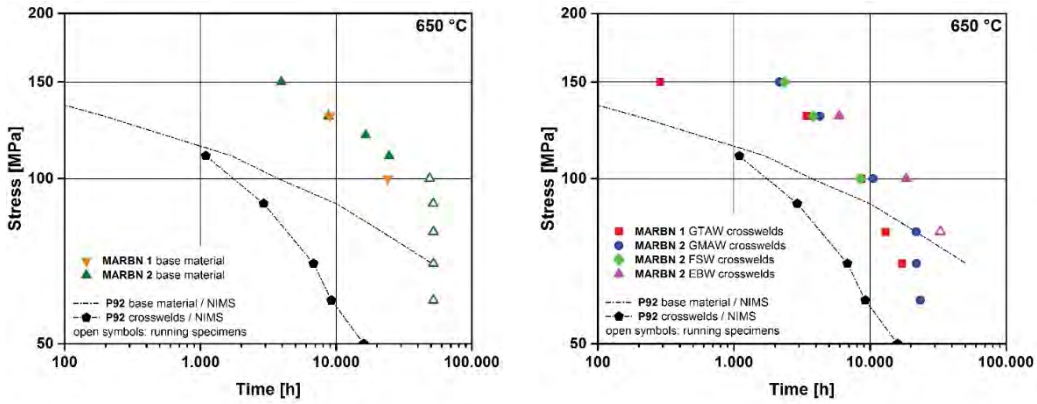


Figure 8: Creep testing data of MARBN 1 and MARBN 2 base material (left) and MARBN 1 and MARBN 2 crosswelds (right) compared to values of P92 base material and welded joints tested at 650 °C [28].

Figure 9 left shows the light optical macrographs of the creep exposed crosswelds at a stress level of 130 MPa. Microstructural investigations show that all crossweld samples failed in the HAZ similar to conventional 9 % Cr crosswelds regardless of the applied welding procedure. Additionally, EBSD investigations of the EBW specimen (Detail 9) clearly show the certain void formation along small grains at the PAGB located in the suppressed FGHAZ. This failure mechanism can be observed at the other crosswelds as well and can therefore be assumed as the main reason for premature creep failures of the MARBN crosswelds. The MARBN concept suppresses the formation of a distinctive FGHAZ successfully due to the mentioned α/γ reverse transformation. However, this concept cannot suppress the formation of fine grains along PAGB leading to a restricted void formation in this area and to the observed failure mechanism. As a conclusion Type IV cracking as a typical failure mechanism of 9-12 % Cr welded joints is still present with regards to MARBN grades but delayed to substantial longer creep durations.

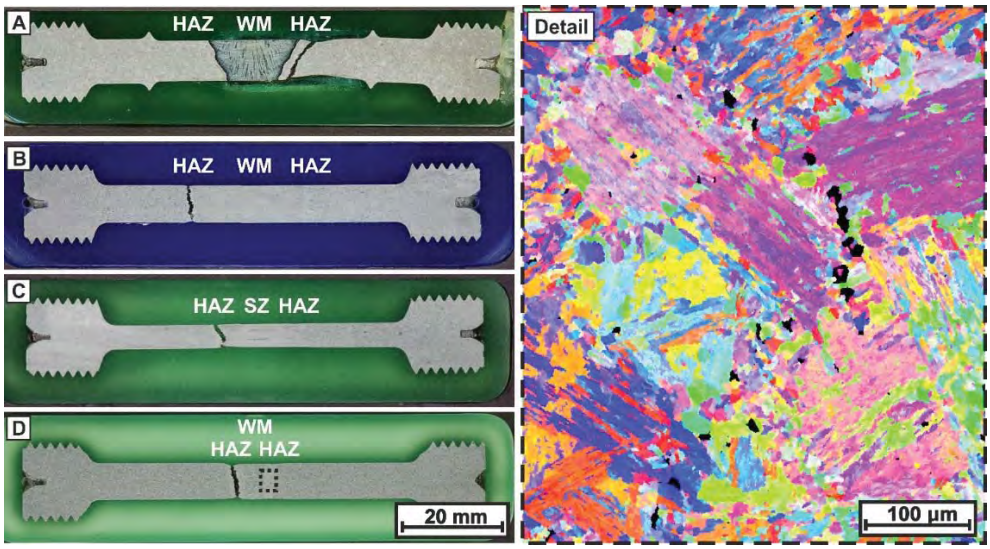


Figure 9: Light optical microscopy images of the creep exposed GTAW crossweld (A), GMAW crossweld (B), FSW crossweld (C), EBW crossweld (D) showing creep failure of the HAZ at 650 °C and 130 MPa (left), and the EBSD measurement of the HAZ of MARBN 2 EBW crossweld (right).

Downloaded from http://dl.asminternational.org/am-epri/proceedings-pdf/AM-EPRI2016/84673/989/678749/epri2016p0989.pdf
by guest

SUMMARY

Within this work, two laboratory heats with controlled boron and nitrogen contents MARBN 1 and MARBN 2 were considered with regards to microstructure, welding behaviour and creep performance summarizing more than 10 years of research. The alloy design philosophy of the MARBN steel grades is based on a boron and nitrogen stabilized martensitic microstructure containing boron enriched $M_{23}(CB)_6$ and vanadium/niobium rich carbonitrides. A strictly balanced boron and nitrogen content is necessary to achieve the beneficial strengthening effect. Both heats exhibit significant improved creep strength compared to well established grade 92 base material at 650 °C. The MARBN 1 base material shows a certain drop in creep strength compared to the MARBN 2 base material at lower stress levels, which was attributed to the existence of boron nitrides due to the slightly higher addition of boron and nitrogen over the solid solubility limit.

Different welding procedures such as GTAW, GMAW, FSW and EBW were applied successfully for both heats showing a suppressed FGHAZ in any case. EBSD measurements revealed small grains aligning at the PAGB instead. Results of the creep performance at 650 °C showed that all crossweld samples could not reach the superior creep strength of MARBN 2 base metal. Nevertheless the overall creep performance of the MARBN crosswelds is still on a much higher level compared to grade 92 welded joints. Especially the EBW crossweld exhibits the best results of all welded joints. The observed improvement of creep rupture strength of the base material and the crosswelds is caused by the effect of decreased precipitate coarsening and the α/γ reverse transformation, which leads to a suppression of the Type IV susceptible FGHAZ during welding. Despite this beneficial effect, premature failures still occur in the HAZ at high stress levels of 130 MPa. EBSD investigations of the superior EBW crossweld showed that the premature failures were caused by certain void formation at the small grains along PAGB in the HAZ. Therefore, Type IV cracking is still present but delayed to substantial longer creep durations due to the MARBN alloy concept.

With regards to the oxidation behaviour the investigated MARBN developed a Cr and Mn rich protective layer which was stable up to at least 20,000 h of exposure to flowing steam at 650 ºC, despite having a Cr content of only 9 wt. %. This results in a superior oxidation behaviour compared to grade 92 steel. Some oxidation nodules were present from the beginning of the test and grew only slowly during exposure. However no new ones appeared to form during the exposure. It is not yet known why this protective oxide forms in this case, since in all other ferritic steels containing 9 wt. % in Cr, a less protective, faster growing oxide scale develops under exposure to steam at 650 ºC.

The strong motivation to enhance steam parameters in fossil power plants in order to increase thermal efficiency leads to a strong demand to develop full size applications of promising high temperature materials for fossil fired power plants such as MARBN steel grades. Due to the sustainable properties and the promising experiences gathered over the last 10 years the MARBN steel grade attracts further attention. Therefore, strong effort was already put into upscaling of these grades to full size demonstration components by several European projects. The European funded MACPLUS project e.g. is targeting on producing melts of several tons as well as first MARBN pipes and welding consumables. The UK project IMPACT which is funded by national government is aiming on further development of research for the energy and power plant industry with MARBN being a certain research topic [30]. Those and many other projects reflect the strong driving force to scale this promising candidate up to future high temperature components.

Downloaded from http://dl.asminternational.org/am-epri/proceedings-pdf/AM-EPRI2016/84673/989/678749/epri2016p0989.pdf
by guest

REFERENCES

[1] World Energy Outlook 2015, International Energy Agency, Paris, France, 2015.

[2] Czyrska-Filemonowicz, A. et al., "Modified 9% Cr steels for advanced power generation: microstructure and properties", Journal of Achievements in Materials and Manufacturing Engineering, Vol. 19, No. 2 (2006), pp. 43-48.

[3] Masuyama, F. et al., "Alloy Development and Material Issues with increasing Steam Temperature", Proc 4th International Conference on Advances in Materials Technology for Fossil Power Plants, Hilton Head Island, South Carolina, 2005, pp. 35-50.

[4] Masuyama, F. et al., "Advanced Power Plant Developments and material Experiences in Japan," Proc 8th Liege Conference on Materials for Advanced Power Engineering, 2006, pp. 157–187.

[5] Abson, D. J. et al., "Review of type IV cracking of weldments in 9-12%Cr creep strength enhanced ferritic steels", Int. Mater. Rev., Vol. 58, No. 8 (2013), pp. 437-473.

[6] Francis, J.A., Mazur, J., Bhadeshia H.K.D.H., "Type IV cracking in ferritic power plant steels", Mater. Sci. Technol., Vol. 22, No. 12 (2006), pp. 1387-1395.

[7] C. Scheu, F. Kauffmann, G. Zies, K. Maile, S. Straub, and K. H. Mayer, "Requirements for microstructural investigations of steels used in modern power plants", Z. Metallkd. 96 (2005) 653-659.

[8] M. Staubli, K.-H Mayer, T.-U. Kern, R.W. Vanstone, R. Hanus, J. Stief, K.-H Schönfeld, "COST 522 - Power Generation into the 21st Century", in: R. Viswanathan, W.T. Bakker, J.D. Parker (Eds.), Proc. Advanced Steam Power Plant, University of Wales and EPRI (2001), pp. 15-32.

[9] Abe, F., „Precipitate design for creep strengthening of 9% Cr tempered martensitic steel for ultra-supercritical power plants" Science and Technology of Advanced Materials, Vol. 9, No 1 (2008),pp. 1-15.

[10] Cerjak, H., "The role of welding in modern power generation plants", Proc. of IIW Int. Conf. on Achievements and perspectives in producing welded construction for urban environments, Bucharest, July 2003, pp. 127-136.

[11] Abe, F. et al, "Mechnism for Boron effect on microstructure and creep strength of ferritic power plant steel", Energy Materials, Vol 4, No.4 (2012), pp166-175.

[12] Li, S. et al, "Microstructural evolution of delta ferrite in SAVE12 steel under heat treatment and short-term creep", Materials Characterization, Vol. 73 (2012), pp. 144-152.

[13] Horiuchi, T., et al, "Improved utilization of added B in 9Cr heat resistant steels containing W", ISIJ Int., Vol. 42, (2002), pp. 67-71.

[14] Kondo, M., et al, "Suppressing type IV failure via modification of heat affected zone microstructures using high boron content in 9Cr heat resistant steel welded joints", Science and Technology of Welding and Joining, Vol. 11, No. 2 (2006), pp. 216-223:

[15] Sommitsch, C., et al., "Co-ordination of European Research in structural Materials for Power Generation Equipment", Proc. 10th Liege Conference: Materials for Advanced Power Engineering, Palais des Congrès Liège, Belgium, 2014, pp. 3-18.

[16] Abe, F., et al., "Creep-resistent steels", Woodhead Publishing, (Abington, 2008), pp. 279-304.

[17] Abe, F., et al., "Suppression of Type IV fracture and improvement of creep strength of 9Cr steel welded joints by boron addition", International Journal of Pressure Vessels and Piping, No. 84 (2007), pp. 44-52.

[18] Mayr, P., "Evolution of microstructure and mechanical properties of the heat affected zone in B-containing 9% chromium steels," Doctoral thesis, Graz University of Technology, 2007.

[19] Abe, F., "Effect of Boron in Creep Deformation Behaviour of 9Cr Steel for USC Boilers at 650 °C", Proc. of the 7th International Charles Parsons Turbine Conference, 2007, pp. 477-488.

Downloaded from http://dl.asminternational.org/am-epri/proceedings-pdf/AM-EPRI2016/84673/989/678749/epri2016p0989.pdf
by guest

[20] Shirane, T.,"Ferrite to austenite reverse transformation process in B containing 9%Cr heat resistant steel HAZ," *Sci. Technol. Weld. Join.*, Vol. 14, No. 8 (2009), pp. 698–707.

[21] Mayr, P., et al., „Boron strenghtening in Ferritic 9Cr3W3CoVNbNB Steel with Improved Crossweld Creep Performance", Proc. 6th International Conference on Advances in Materials Technology for Fossil Power Plants, Santa Fe, New Mexico, 2010, pp. 640-653.

[22] Abe, F., "Creep Deformation Behaviour and Alloy Design Philosophy of Creep-Resistant Tempered Martensitic 9Cr Steel", Proc. 6th International Conference on Advances in Materials Technology for Fossil Power Plants, Santa Fe, New Mexico, 2010, pp. 620-639.

[23] Agüero, A., González, V., Mayr, P., Spiradek-Hahn, K., Anomalous Steam Oxidation Behaviour of a Creep Resistant Martensitic 9 wt. % Cr Steel, Materials Chemistry and Physics, 141 432 (2013).

[24] Agüero, A., González, V., Gutiérrez, M., Muelas, R., Oxidation Under Pure Steam: Cr Based Protective Oxides and Coatings, Surface & Coating Technologies. 237, 30 (2013).

[25] Quadakkers, W.J., Ennis, P.J., The Oxidation Behaviour of Ferritic and Austenitic Steels in Simulated Power Plant Service Environments, Materials for Advanced Power Engineering 1998, I, 123 (1998).

[26] National Institute for Materials Science, "NIMS Creep Data sheet no. 48A," Tsukuba, Japan, 2012.

[27] Schlacher, C., Béal, C., Sommitsch, C., Mitsche, S., Mayr, P. "Creep and damage investigation of advanced martensitic chromium steel weldments for high temperature applications in thermal power plants," Sci. Technol. Weld. Join., vol. 20, no.1 (2015), pp. 82–90.

[28] Schlacher, C., Untersuchung des Kriech- und Schädigungsverhaltens von Schweißverbindungen eines mertensitischen borlgeierten 9%Cr-Stahls", Doctoral thesis, Graz University of Technology, 2015.

[29] Abe, F., Tabuchi, M., Tsukamoto, S., Liu, Y. "Alloy design of tempered martensitic 9Crboron steel for A-USC boilers," in *Advances in Materials Technology for Fossil Power Plants: Proceedings from the Seventh International Conference*, 2014, pp. 1127–1138.

[30] Sommitisch, C., et al, „Co-ordination of European Reseach in Structural Materials for Power Generation Equipment", Proc 10th Conference of Materials for Advanced Power Engineering, Juelich, Germany, 2014, pp. 3-18.

Downloaded from http://dl.asminternational.org/am-epri/proceedings-pdf/AM-EPRI2016/84673/989/678749/epri2016p0989.pdf
by guest